Electrical equivalent circuit for air and liquid characterization of a multilayer micromembrane with piezoelectric actuation and read-out capabilities

T.Alava, C.Ayela and L.Nicu

Laboratory of Analysis and Architecture of Systems, CNRS, Toulouse, FRANCE, alava@laas.fr

ABSTRACT

This paper presents the elaboration of an analytical model for a resonating micromembrane. The membranes are dedicated to biosensing experiments, the actuation and detection being realized by the action of a lead zirconate titanate 46/54 $PbZr_xTi_{1-x}O_3$ piezoelectric material cell. The model is synthesized as an equivalent Butterworth-Van-Dyke circuit enabling the direct modelling of the membranes' behaviour both in air and a viscous fluid. The model is established for a five layer stack micromembrane mounted with a circular piezoelectric cell. The fabrication of membranes with a global radius of 100 µm and different piezoelectric cell sizes is reported. The characteristics curves for the membranes behaviour are extracted for the vibrations in air and in water. The comparison of theoretical and experimental results is detailed and reveals a good accordance between the modelled and the extracted curves.

Keywords: piezoelectric thin film, multilayer micro-membrane, integrated actuation, integrated read-out

1 INTRODUCTION

In the past few years, microresonators have shown a great interest in the field of micro electro mechanical systems (MEMS) especially for biosensing applications. In the scope of this paper, the case of a piezoelectrically actuated and read-out resonating micromembrane is treated. In order to acquire a deeper knowledge of micromembranes resonators a set of differential equations has to be solved, either numerically or analytically. The numerical method, based on FEA (Finite Elements Analysis), still widespread, is highly time- consuming for complex structures. To gain over calculation time, research has been lead to develop "equivalent circuits model" based on an analogy between electrical and mechanical domains. Tilmans [1] have already reported a general study of such approaches for MEMS. In this paper, we report the elaboration of a Butterworth-Van Dyke (BVD) equivalent circuit for a piezoelectrically actuated and read-out resonating micromembrane. Following a previously lead study by DeVoe [2], the electrical components were extracted from the mechanical characteristics of the membrane for vibrations in air an in liquid. The elaborated model was then compared to the experimental results extracted from the membranes.

2 EQUIVALENT CIRCUIT MODELLING FOR THE PIEZOELECTRIC MEMBRANE

The membrane is constituted by a five layer stack and has a circular shape (Layer details and geometry are, respectively detailed in fig 1. and tab 2.). The actuation and sensing functions are performed by a lead zirconate titanate 46/54 $PbZr_xTi_{1-x}O_3$ (PZT) thin film.

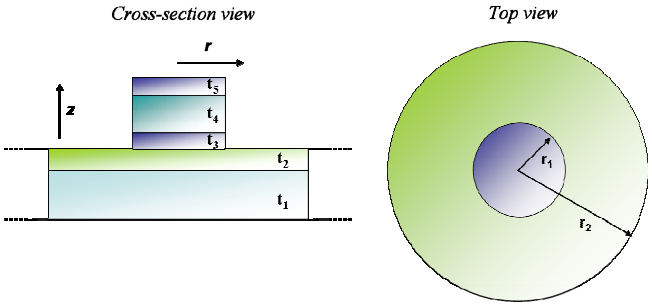

Figure 1: Detail of the five-layer stack structure of the micromembranes

Layer	Thickness
Silicon	t_1 = 2 µm
Silicon dioxide	t_2 = 250 nm
Bottom platinum electrode	t_3 = 100 nm
PZT	t_4 = 1 µm
Top platinum electrode	t_5 = 100 nm

Outer radius (R_2)	Ratio (R_1/R_2)	Inner radius (R_1)
100 µm	0.3	30 µm
	0.5	50 µm
	0.7	70 µm

Table 1: Main geometrical parameters of a resonating micromembrane with piezoelectric actuation and detection

The application of an input voltage to the piezoelectric thin film induces the deflection of the membrane. The related deflection of the vibrating membrane is overcome by the piezoelectric layer implying a current generation in the output circuit. As depicted in fig. 2 the membrane plus its actuation and read-out apparatus has to be modelled as a global admittance.

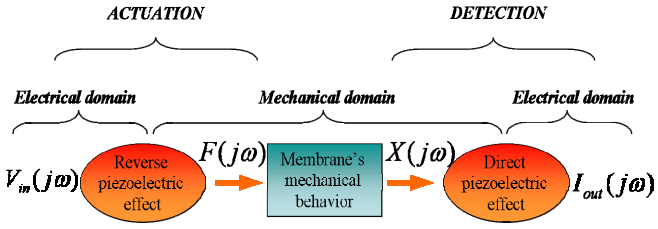

Figure 2: Overview of a piezoelectrically actuated and read-out membrane working principle

Introducing two coupling coefficients, the transfer function modelling the membrane's global admittance has been divided into three parts:

$$H(j\omega)=\frac{I_{out}(j\omega)}{V_{in}(j\omega)}=(j\omega)\frac{X(j\omega)}{F(j\omega)}\eta_1\eta_2 \quad (1)$$

With η_1 being the *actuation coupling coefficient*, equals to $\frac{F(j\omega)}{V_{in}(j\omega)}$ and η_2, equals to $\frac{1}{j\omega}\frac{I_{out}(j\omega)}{X(j\omega)}$, being the *sensing coupling coefficient*

2.1 Coupling coefficients

In order to compute the coupling coefficients, following an analogy to the work previously lead by DeVoe [2] , the fundamentals equations of piezoelectricity were combined to the expression of output current and to the exerted force on the membrane. In this study, the initial residual stress in the membrane and all shear effects were neglected. The equations of piezoelectricity were modified according to the bi-dimensionality of the membrane problem:

$$S_1=(s_{11}^E+s_{12}^E)T_1+d_{31}E_3 \quad (2)$$

$$D_3=2d_{31}T_1+\varepsilon_{33}^T E_3 \quad (3)$$

S_1 and T_1 are respectively the strain and the stress along the x-direction. D_3 represents the electrical displacement in the film along the z-direction while E_3 corresponds to the electric field across the PZT film. d_{31} is the piezoelectric coefficient coupling the electric field in the z-direction and the related strain in the x-direction. s_{11}^E and s_{12}^E are the mechanical compliances in the x-y plane and ε_{33}^T is the permittivity of the material.

The shift between the PZT film and the neutral plane of the membrane (i.e. the plane where the stresses contribution of all the layers are considered null) implies that the deflection of the piezoelectric film generates a bending moment. The shear load on the membrane has been neglected in the calculations. Thus, the modal force for a determined vibration mode is given by

$$P_{tot}(\theta)=\int_0^{r_2}P(r,\theta)\phi_{mn}(r,\theta)dr \quad (4)$$

where $P(r,\theta)$ represents the distributed load on the membrane; it is linked to the bending moment as it second derivate. The moment force depends directly from T_1, the stress along the x-axis in the piezoelectric material. $\phi_{mn}(r,\theta)$ represents the mode shape for the mode (m,n) of vibration. In this study, only the fundamental mode (0,0) is considered. The formulas for the mode shape were found in [3]. Therefore, combining the fundamentals equations of piezoelectricity and the equation (4), the expression of the modal force exerted on the membrane have been obtained, depending on T_1 and consequently on E_3, the electrical field in the piezoelectric material. The electrical field in the PZT thin film along the z-direction has been chosen as the applied voltage divided by the PZT layer thickness. Finally, the driving coupling coefficient is determined:

$$\eta_1(\theta)=-2\pi\frac{d_{31}}{s_{11}^E+s_{12}^E}z_{2Pt\,\mathrm{inf}}\left[r_1\phi'_{mn}(r_1,\theta)-\phi_{mn}(r_1,\theta)\right] \quad (5)$$

with $\phi'_{mn}(r_1,\theta)$ representing the derivate of the mode shape function regarding the radial coordinate. Z_{2Ptinf} is the distance of the inferior Pt electrode from the neutral plane.

In order to determine the sensing coupling coefficient the value of the output current (due to the charges generated in the piezoelectric material) has been determined by integrating over the whole sense electrode surface the piezoelectrically-induced charges per unit area, represented by D_3:

$$I_{out}=j\omega\iint_S D_3 \quad (6)$$

S being the surface of the sense electrode. The expression of D_3 can be determined as a function of the strain S_1, combining (2) and (3). Here, the extensional strain and therefore the influence of d_{33}, have been neglected.

Computation of equation (6) has given:

$$I_{out}=j\omega\frac{4\pi\, d_{31}}{s_{11}^E+s_{12}^E}z_{2Pt\,\mathrm{inf}}\bar{y}[\phi_{mn}(r_1,\theta)-\phi_{mn}(0,\theta)-r_1\phi'_{mn}(r_1,\theta)]+j\omega V_{in}\,C_{static} \quad (7)$$

Introducing the static capacitance of the piezoelectric patch

$$C_{static}=\frac{\pi\, r_1^2}{t_{PZT}}\left(\varepsilon_{33}^T-\frac{2d_{31}^2}{s_{11}^E+s_{12}^E}\right). \quad (8)$$

Due to the ferroelectricity of the PZT material, the input voltage causes a steady current (linked to the static capacitance) to superimpose to the oscillating part of the output current. As only this oscillating part contains information on the vibratory state of the membrane, a new definition for the sensing coupling coefficient is introduced, knowing the steady part of the output current will have to be taken into account further.

NSTI-Nanotech 2007, www.nsti.org, ISBN 1420061844 Vol. 3, 2007

$$\eta_2(\theta) = \frac{1}{j\omega}\frac{I_{out} - I_{static}}{\bar{y}} = \frac{4\pi\, d_{31}}{s_{11}^E + s_{12}^E} z_{2Pt\,\inf}\left[\phi_{mn}(r_1,\theta) - \phi_{mn}(0,\theta) - r_1\phi'_{mn}(r_1,\theta)\right] \quad (9)$$

2.2 Admittance

Once the two coupling coefficients determined, the mechanical transfer function of the membrane is determined from a simple second order differential equation describing the membrane's dynamic behavior.

$$\frac{X(j\omega)}{F(j\omega)} = \frac{1}{j\omega}\frac{1}{\xi_{eff} + \frac{K_{eff}}{j\omega} + j\omega M_{eff}} \quad (10)$$

To model the global admittance of the membrane plus the actuation and sensing system, one will have to divide equation (10) by both coupling coefficients and to introduce the equivalent resistance, capacitance and inductance. At last, it's necessary to take into account the static contribution to output current due to the static capacitance.

$$H(j\omega) = \frac{I_{global}(\omega)}{V_{in}(\omega)} = \frac{I_{global}(\omega) - I_{static}(\omega)}{V_{in}(\omega)} + j\omega C_{stat}$$

$$H(j\omega) = \frac{j\omega(C_{eq} + C_{stat}) - \omega^2 C_{eq} C_{stat} R_{eq} - j\omega^3 L_{eq} C_{eq} C_{stat}}{1 - \omega^2 L_{eq} C_{eq} + j\omega C_{eq} R_{eq}}$$

With: $L_{eq} = \frac{M_{eff}}{\eta_1\eta_2}$ $C_{eq} = \frac{\eta_1\eta_2}{K_{eff}}$ $R_{eq} = \frac{\xi_{eff}}{\eta_1\eta_2}$

The circuit governed by this transfer function is showed fig 2.

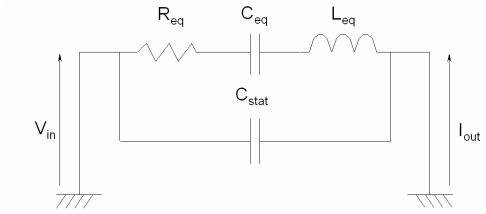

Figure 2: Representation of the equivalent electrical circuit modeling the dynamic behavior in air of the membrane with piezoelectric actuation and read-out.

2.3 Admittance modeling in liquid

The presence of surrounding fluid has an impact on the membrane's mechanical characteristics leaving unchanged actuation and detection, therefore only the core of the model shall be modified. Two forces are undergone by the membrane vibrating in a viscous fluid: on one hand, a force proportional to the membrane velocity (the fluid damping force) and on the other hand, a force proportional to the membrane acceleration (linked to the mass of fluid remaining stuck on the membrane during the vibrations). So, a direct way to model the effect of fluid is to add in the serial branch of the equivalent electrical circuit, an extra fluidic resistance and an extra fluidic inductance. The resulting circuit can be shown fig 3.

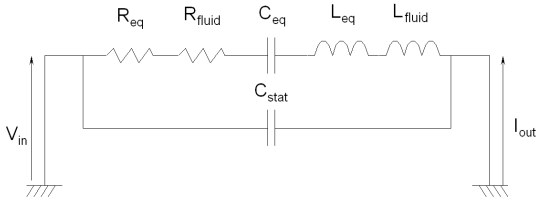

Figure 3: Equivalent electrical circuit modelling the membrane's dynamic behaviour in a viscous fluid.

The value for both fluidic elements have been calculated from a model proposed by Lamb [4] introducing β, usually called added virtual mass incremental (AVMI) factor, is equal to:

$$\beta = 0.67\frac{\rho_L R}{\rho_M h} \quad (12)$$

with ρ_M and h respectively the density and the thickness of the membrane. The fluidic impedances were calculated as:

$$L_{fluid} = \beta\, L_{eq} \quad \text{and} \quad R_{fluid} = \frac{\omega_0 L_{eq}}{Q_{fluid}}\sqrt{1+\beta} \quad (13)$$

3 FABRICATIONS AND RESULTS

The membranes have a circular shape with a global radius of 100 μm. The PZT circular cell used for actuation and sensing was superimposed upon the membrane. The process fabrication has been described in details in previous work [5]. Experimental resonant frequencies and quality factors were calculated from the extracted susceptance and conductance curves (corresponding respectively to the real and imaginary parts of admittance). The complete experimental results for testing in air and water are displayed table 2. The model results for the membranes with a 30 µm radius actuation cell, though in agreement for the resonance frequency, exhibit a great discrepancy with experience in term of amplitude at resonance in air. Moreover for the case of water the theoretical resonance frequency is shifted up from the experimental one by 28%. The simulated curves for the membranes with a 50 µm radius PZT patch are in agreement with experience in term of frequency. The discrepancy in term of amplitude is about six times less important than for the membranes with a 30 µm PZT patch. In liquid the discrepancy in amplitude is equivalent. However, though the frequency behavior is comparable, the curves in liquid show a 18% shift in frequency.

In the case of the membranes with a PZT patch of 70µm in radius, the model has revealed a very interesting correspondence with experience, as shown on figure 6.

Active cell radius (µm)	Air environment		Water environment	
	Experience			
	Resonant frequency in air (*k*Hz)	Resonant frequency in water (*k*Hz)	Quality factor in air	Quality factor in liquid
30	580.5	234.89	208.2	108
50	584.21 ± 48.71	250.48 ± 22.05	252.6 ± 25.4	122 ± 35.4
70	532.29 ± 75.67	237.85 ± 39.53	266.4 ± 0.85	152 ± 1.4
	Theory			
	Theoretical resonant frequency (*k*Hz)	Resonant freq. error	Theory/experience amplitude ratio	Theoretical resonant frequency (*k*Hz)	Resonant freq. error	Theory/experience amplitude ratio
30	580.9	0.06%	174.4	170.418	27.44%	102.7
50	584.143 ± 42.07	0.01%	30.37 ± 5.72	212.73 ± 25.95	15.07%	36.15 ± 2.69
70	532.92 ± 73.98	0.12%	3.87 ± 3.58	212.38 ± 40.22	10.71%	3.42 ± 2.73

Table 2: Detailed presentation of experimental results and of the comparison between theory and experience results.

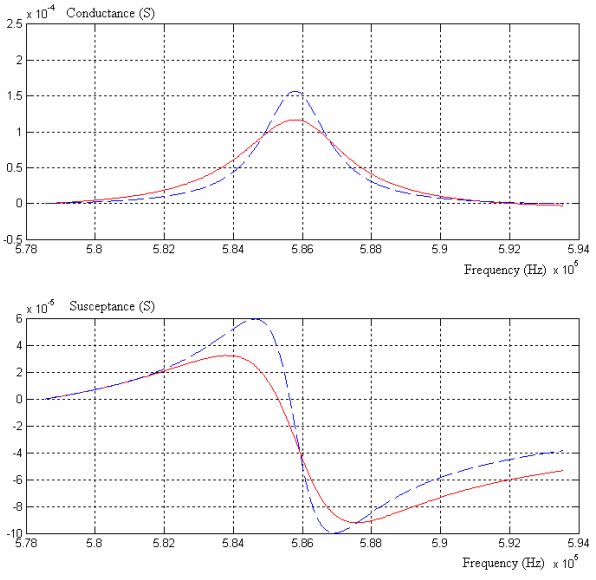

Figure 6: Comparison of the theoretical and experimental curves of conductance and susceptance for a membrane with an active cell of 70 µm. Respectively, the experimental and theoretical curves are represented on the graph by a red solid line and a blue dashed line

Results for theses membranes tested in air and water are shown table 2. In this case, the dynamic behaviour of the membranes has revealed a low discrepancy in resonance's peak amplitude (ratio between theoretical and experimental amplitude is about 3). Concerning the vibrations in water, the correspondence is as good as in air but the theoretical curve is shifted in frequency by a quantity equal to 10% of the experimental resonance frequency value.

The inputs data allowing the equivalent electrical circuit model to compute results are the geometrical parameters (described in table 1) of the membranes. Both for air and water, values for the quality factors were chosen equals to the ones extracted directly from the resonance curves of each tested membrane.

Comparing the theoretical and experimental resonant frequencies in air, the results were in good agreement, with low changes of the geometrical parameters, as shown in table 2. In the case of liquid, discrepancies decreased when the radius of the active cell increased, with a 10% error between the theoretical and the obtained experimental resonant frequency for the membranes with a PZT patch of 70 µm in radius. This is mainly due to the assumption of the Lamb's model. Indeed, no size dependence of the active cell could be taken into account, this model having been established for a homogeneous circular plate. However, the comparable theoretical and experimental values confirmed the reliability of the electrical modelling of the structures vibrating in air and liquid.

4 CONCLUSION

A global analytical model allowing the simulation of the vibrations in air and in liquid of micromembranes with piezoelectric actuation and detection has been established. Membranes with a 100 μm global radius, using a 54/46 $Pb(Zr_xTi_{1-x})O_3$ piezoelectric material, were fabricated and tested. Resonant frequencies ranging from 532 *k*Hz to 584 *k*Hz were measured in air depending on the size of the membrane's actuation cell; in water resonant frequencies ranging from 208 *k*Hz to 266 *k*Hz were measured. Theoretical results extracted from the model were compared to experience. Good accordance was observed in air for the membranes with an actuation cell of 70 μm. Discrepancies in amplitude at resonance peak were observed for the other membranes vibrating in air. Immersed in a viscous fluid, the same discrepancies were observed with a shift in frequency of the theoretical curves towards lower values when compared to the experimental ones.

REFERENCES

[1] H.A.C. Tilmans, J. Micromech. Microeng., 7, 285-309, 1997

[2] D.L. DeVoe, "Thin Film Zinc Oxide Microsensors and Microactuators," PhD Dissertation, University of California Berkeley CA, 1997

[3] R.D. Blevins, "Formulas for natural frequency and mode shape," Krieger Publishing Company, 1995

[4] H. Lamb, "On the vibrations of an elastic plate in contact with water," Proc. Royal Soc. London A, 98, 205-216, 1920.

[5] C. Ayela, L. Nicu, C. Soyer, E. Cattan and C. Bergaud, J. Appl. Phys., 100, 054908-1 – 054908-9, 2006.